

Anatomic and functional evaluation of the lymphatics and lymph nodes in diagnosis of lymphatic circulation disorders with contrast magnetic resonance lymphangiography

Ning-Fei Liu, MD, PhD,^a Qing Lu, MD,^b Zhao-Hua Jiang, MD, PhD,^a Chen-Guang Wang, MD, PhD,^c and Jian-Guo Zhou, MD,^a *Shanghai, China*

Objectives: Owing to its structural and anatomic characteristics, imaging of the lymphatic system has been difficult. The conventional diagnostic method of radionuclide-based imaging has the disadvantage of poor resolution. Recent work has shown that magnetic resonance imaging (MRI) can depict lymphatic channels in patients with lymphedema. This study evaluated the anatomic and functional images of contrast MR lymphangiography in the diagnosis of limb lymphatic circulation disorders.

Methods: The study enrolled 27 patients with primary lymphedema. Four patients had bilateral disease, and 23 had unilateral disease. Contrast-enhanced lymphangiography was performed with a 3.0-T MR unit after the intracutaneous injection of gadobenate dimeglumine into the interdigital webs of the dorsal foot. The kinetics of enhanced lymph flow within the lymphatic system were calculated using the formula [speed in cm = total length of visualized lymph vessel in cm/inspection time in minutes] and by comparing dynamic nodal enhancement and time-signal intensity curves between edematous and contralateral limbs. Morphologic abnormalities of the lymphatic system were also evaluated.

Results: Examination of the MRIs after injection of the contrast agent showed enhanced lymphatic channels consistently visualized in all clinical lymphedematous limbs and in five contralateral limbs of unilateral lymphedema patients. The speed of flow within the lymphatics of lymphedematous limbs was 0.3 to 1.48 cm/min. Contrast enhancement in inguinal nodes of edematous limbs was significantly less than that of contralateral limbs ($P < .01$). Dynamic measurement of contrast enhancement showed a remarkable lowering of peak time ($P < .01$) and peak enhancement ($P < .01$), and a delay in outflow in inguinal nodes of affected limbs compared with that of control limbs. Postcontrast MRI also depicted varied distribution patterns of lymphatics and abnormal lymph flow pathways within lymph nodes in the limbs with lymphatic circulation disorders.

Conclusion: Contrast MR lymphangiography with gadobenate dimeglumine is capable of visualizing the precise anatomy of lymphatic vessels and lymph nodes in lymphedematous limbs. It also provides information concerning the functional status of lymph flow transport in the lymphatic vessels and lymph nodes of these limbs. (*J Vasc Surg* 2009;49:980-7.)

The development of clinical lymphology was slow for many years. This was largely due to the lack of optimal diagnostic methods for assessing lymphatic diseases, including lymphatic system imaging. Lymphoscintigraphy using isotopic contrast agents does not have sufficient resolution to accurately outline the internal anatomy of lymph nodes and lymphatic vessels. The measurement of tracer clearance from the injection point and accumulation of tracer in the inguinal lymph node may be valuable in functional analysis, but it has limited diagnostic accuracy.

In addition, direct lymphangiography using an iodine oil agent that is capable of visualizing the lymphatics is no longer routinely performed because it can lead to life-threatening complications and is difficult to perform. Furthermore, neither method can be used to make a dynamic observation of the lymphatic system and lymph nodes. It is, therefore, essential to find an imaging modality that in addition to mapping the anatomic distribution of the affected lymphatic system is also capable of defining its function.

Magnetic resonance imaging (MRI) has been used in our clinic for diagnosis of lymphatic disorders^{1,2} since 1990. MRI has a number of potential advantages compared with lymphoscintigraphy, including higher spatial resolution enabling depiction of lymphatic channels, higher temporal resolution, production of three-dimensional (3D) images, and the absence of exposure to ionizing radiation. In recent years, a number of different contrast agents have also been developed and tested in MR lymphangiography for imaging of the lymphatic system.³⁻⁷ Most of these agents are intravenously injected for the staging of malignant lymph nodes or to show lymphatic drainage patterns.

From the Department of Plastic and Reconstructive Surgery, Shanghai 9th People's Hospital, Shanghai Jiao Tong University School of Medicine^a; the Department of Radiology, Shanghai Ren Ji Hospital, Shanghai Jiao Tong University School of Medicine^b; and the Department of Radiology, Shanghai Chang Zheng Hospital, Second Military Medical University.^c This study was sponsored by Shanghai Science and Technology Committee (0541195361).

Competition of interest: none.

Reprint requests: Ning-Fei Liu, MD, Department of Plastic and Reconstructive Surgery, Shanghai 9th People's Hospital, 639 Zhi Zao Ju Rd, Shanghai 200011, China (e-mail: liuningfei@126.com).

0741-5214/\$36.00

Copyright © 2009 by The Society for Vascular Surgery.

doi:10.1016/j.jvs.2008.11.029

We report the results of contrast MR lymphangiography after the intracutaneous injection of gadobenate dimeglumine in patients with benign lymphatic circulation disorders of the extremities. To our knowledge, this is the first report of the usefulness of dynamic MR lymphangiography in the imaging of the lymphatic system in human limbs with lymphatic circulation disorders.

METHODS

Patients. The present study included 27 patients (17 males, 10 females) with a mean age 28 of years (range, 8-75 years) and a mean duration of disease of 7.8 years (range, 4 months-28 years). Among them, four had stage I lymphedema, which represents an early accumulation of fluid that subsides with limb elevation, and the remainder had stage II disease, which signifies tissue swelling that is rarely reduced by limb elevation alone and some degree of tissue fibrosis in the limb.

Contrast. The contrast agent used for MR lymphangiography in this study is the commercially available and widely used paramagnetic contrast medium gadobenate dimeglumine (Gd-BOPTA, MultiHance, Bracco, Milan, Italy). Before injection, 1% lidocaine (1.5 mL) was added to each bottle of gadobenate dimeglumine (15 mL), and the mixed agent was injected intracutaneously into the interdigital webs of the dorsal foot, with four injections in each limb. The volume injected into each point was 0.7 to 0.8 mL.

Dynamic 3D-MR lymphangiography. All MR examinations were performed with a 3.0-T MR unit (Philips Medical System, Best, The Netherlands) with a maximum gradient strength of 80 mT/m and a slew rate of 200 mT/m/ms. Patients were supine. A six-element phased-array sensitivity encoding cardiac reception coil was used. The scanning was started from the patient's foot and moved towards the inguinal region in three or four separate and successive inspections according to length of the body.

Before injection of the contrast agent, a 3D heavily T2-weighted MRI was performed. The serial turbo sequences included fat saturation and half-scan acquisition, single-shot fast spin-echo sequence. The repetition time (TR) was 2820 milliseconds, the echo time (TE) was 740 milliseconds, field of view (FOV) was 360×285 mm, matrix was 240×190 , and slice thickness was 2 mm, with 55 to 85 slices produced. A series of maximum intensity projection (MIP) images were reconstructed. For dynamic MR lymphangiography, 3D fast spoiled gradient-recalled echo T1-weighted images with a fat saturation technique (T1 high-resolution isotropic volume excitation) were acquired at 5, 10, 15, 20, 25, and 30 minutes after contrast injection. The MR imaging parameters were TR/TE, 3.5/1.7 milliseconds; flip angle, 25°; FOV, 360×320 mm; matrix, 300×256 ; slices, 55 to 95; voxel size, $1.5 \times 1.2 \times 1.2$ mm; signal average number, 2; and acquisition time, 0 min 40 seconds.

The 3D MRIs were then reconstructed from the post-contrast coronal images at each time point using an MIP technique. The examination time for one patient was ap-

proximately 1.5 hours. No systemic or local complications were observed during or after the examination.

Image interpretation and data analysis. The contrast enhancement of the lymph vessels and lymph nodes of the lower extremities and inguinal region was qualitatively and quantitatively evaluated independently by two observers. The appearance and distribution pattern of the lymphatic pathway in the diseased extremities and the morphologic characteristics of the inguinal nodes on the MRIs before and after contrast were analyzed. The existence and location of edema in the affected limbs were evaluated. A quantitative analysis was also performed, including:

1. Assessment of the time course of enhancement of lymph flow in vessels directly draining from the injection sites. After contrast injection, the measurement of contrast movement in a contrast-enhanced lymphatic vessel was assessed from the ankle region along its course towards the proximal leg in a series of five to six successive images along the enhanced lymph vessel with a clear outline. The length of the enhanced vessel on the final image was recorded and the speed of contrast movement was calculated using the formula [speed in cm = total length of visualized lymph vessel in cm/ inspection time in minutes].
2. Assessment of enhancement of inguinal lymph nodes directly draining from the injection sites. For evaluating these results, the ratio of signal intensity (SI) of the lymph node against the SI of adjacent muscle was estimated. The operator-defined regions of interest (ROIs) were drawn on the coronal postcontrast images. At least of one pair of inguinal nodes was measured. The ROI on muscles was selected in the upper portion of the thigh near the inguinal region with lymph nodes that were approximately the same size. The ratio of node/muscle SI was compared between lymphedematous and contralateral limbs on postcontrast MRIs. For each patient, the dynamic enhancement of contrast in the bilateral nodes was estimated, the wash-in and wash-out curves were derived from designated ROIs, and the peak enhancement time and lymph node/muscle SI ratio at peak time were directly compared.

Statistical analysis. All results were expressed as means with standard deviations. The paired *t* test was used to compare the significance of the differences between mean values. A value of $P < .05$ was taken to indicate a significant difference.

RESULTS

Lymphatic system imaging

Lymphatic drainage patterns. Contrast enhancement of the lymphatic system was seen soon after contrast injection, and the contrast agent generated clear images of the lymphatic vessels and lymph nodes with a low background. On the postcontrast MRIs, consistently enhanced images of the lymphatic channel were visualized in all lymphedematous limbs, although contrast-enhanced lymph-

phatic vessels could not be visualized in the limbs of two healthy volunteers. However, contrast-enhanced lymphatic vessels could be seen in five contralateral nonedematous limbs of the 23 patients with unilateral primary lymphedema. The contrast enhancement of these lymphatic pathways persisted for about 40 minutes during the examination. The initial images the enhancement of lymphatic channels was light and discontinuous in some cases; however, the SI increased and the channels gradually become totally opacified with time. No leakage of contrast from the lymphatic vessels was seen, but dermal backflow was observed the distal part of the leg and foot in three patients.

The number of contrast-enhanced lymphatic vessels in the primary lymphedematous limbs varied from a single vessel to numerous vessels, and lymphatic vessels that could be visualized had diameters of 1.2 to 8 mm. Lymphatic vessels in edematous limbs were also irregularly shaped, had an uneven diameter or were twisted, and could be easily distinguished from venous vessels. Patterns seen in the lymphatic pathways of patients with primary lymphedema included:

- numerous tiny skin lymphatic vessels and dermal backflow in the lower part of the leg, plus one or two dilated lymphatic collectors in the upper part of the leg (Fig 1, *a*);
- radiating, enhanced vessels in lower leg that assembled at the medial portion of the knee and went up to the thigh (Fig 1, *b*);
- discontinuous and lightly enhanced but dilated vessels in the medial portion of the lower limb (Fig 1, *c*);
- bunches of extremely dilated and significantly enhanced lymphatic vessels located mainly in the medial and, to a lesser extent, the lateral portion of the thigh (Fig 1, *d*); and
- remarkably dilated and opacified lymphatic vessels that went from the lower leg directly to the inguinal node with few branches (Fig 1, *e* and *f*).

Fine afferent and efferent lymph vessels between the superficial and deep groups of inguinal nodes were also clearly visualized in some limbs.

The MRIs also provided information on extralymphatic changes by showing the location and extent of edema fluid. Indeed, accumulation of edema fluid in subcutaneous tissue and contrast-enhanced lymphatic vessels could be visualized in all 27 patients with primary lymphedema.

Contrast transportation in lymphatic channels.

Contrast-enhanced lymph flow speed was measured in 25 patients; among them, 23 limbs in 20 patients were available for dynamic observation of the contrast-enhanced flow at a series of time points. The speed of the enhanced lymph flow was 0.3 to 1.48 cm/min (Fig 2, *b*), and the mean flow speed of the lymph vessels at each time point in the 23 limbs is shown in Fig 2, *c*.

Possible correlations between the transporting capabilities of these vessels and their diameter, the number of lymphatic vessels in each affected limb, and disease duration were compared. The speed of enhanced lymph flow was compared between subgroups of vessel diameters (10 at <2

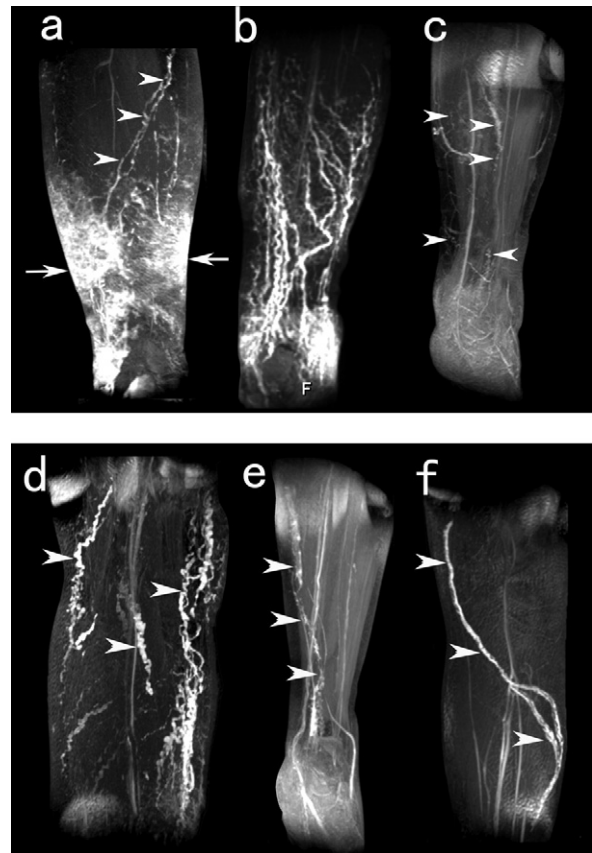


Fig 1. A 3-dimensional contrast magnetic resonance lymphangiography displayed various lymphatic drainage pathways. **a**, Increased skin lymphatic and dermal back-flow in the medial and lateral region of lower leg (*arrow*) and dilated collectors in the upper part of leg (*arrowhead*). **b**, Radiating arranged dilated vessels in the lower leg of primary lymphedema cases. **c**, Enhanced lymphatic vessels (*arrowheads*) distributed as a slender network over the lower extremity. **d**, Bunches of extremely dilated and significantly highlighted lymphatic vessels (*arrowheads*) located in the medial and lateral portion of the thigh. **e**, Single enhanced and dilated lymphatic (*arrowheads*) with irregular outline in the leg of primary lymphedema. **f**, An intensely enhanced dilated lymph vessel (*arrowheads*) with clear outline in the thigh.

mm, 16 at 2 to 5 mm, and 6 at 5 to 8 mm), numbers of visualized lymphatic vessels (10 with 1 to 2; 9 with 3 to 20; and 6 with >20), and lymphedema duration (6 at <1 year; 11 at 2 to 5 years; and 10 at >5 years). No significant differences were found in enhanced flow speed between the vessels with different diameters or between subgroups with different disease duration.

Furthermore, the observed kinetic result of lymph flow in an individual vessel did not appear related to the numbers of lymphatic vessels in the affected limbs (Fig 2, *d*). However, we noted that the speed of lymph transport might depend on the individual patient; for example, in one patient with primary lymphedema in the left lower extremity of >20 years, the tested speed of flow was 1.25 cm/min,

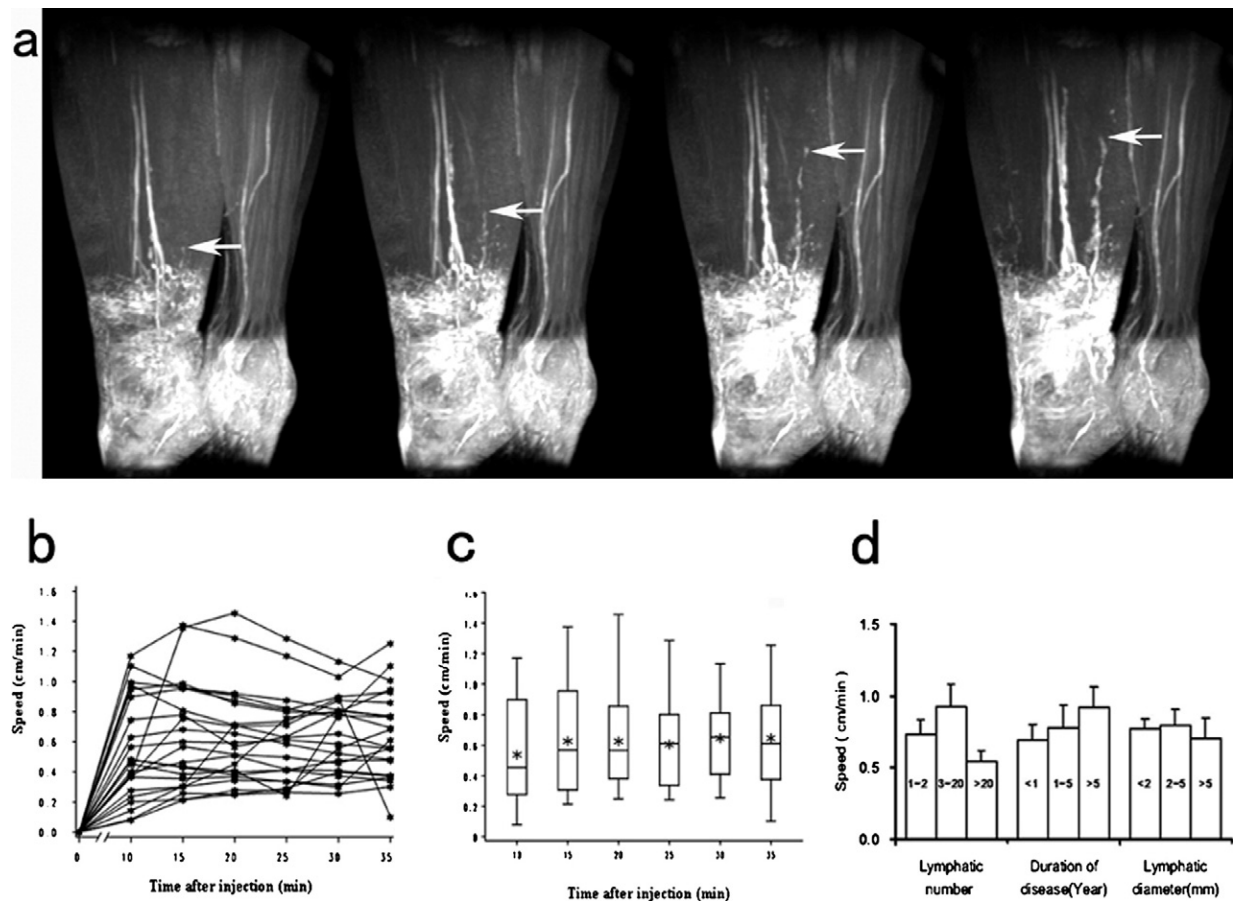


Fig 2. Dynamic images of enhanced lymph flow. **a**, Observation of movement of contrast-enhanced flow in a lymphedematous limb. **b**, Enhanced flow speed (cm/min) at a series time points is shown for of 23 lymph vessels of lymphedematous limbs. **c**, Mean flow speed is charted at each time point of 23 tested vessels. * The horizontal line in the middle of each box indicates the median; the top and bottom borders of the box mark the 75th and 25th percentiles, respectively. The whiskers mark the 90th and 10th percentiles. **d**, Comparison of lymph speed in three groups with various vascular diameters, vascular numbers and disease durations. Data are presented with the standard deviation.

which was among the highest scores of those patients in this study. The diameter of the imaged vessels in the patient was 6.1 mm, which was also within the highest range in the study (Fig 1, f).

Lymph node imaging

Morphologic characteristics of the inguinal lymph nodes. The morphologic changes, including nodal size, internal lymph node architecture, and lymph node borders, were also evaluated. The shape of the inguinal lymph node on the contralateral side in patients with lymphedema and in healthy volunteers was spherical or oval, and inguinal nodes in these patients numbered from 2 or 3 to 7 or 8, with a diameter of approximately 1.0 cm. In contrast, large variation was noted in the outline, number, and volume of inguinal nodes in primary lymphedematous extremities. Compared with contralateral limbs, the abnormalities of inguinal nodes in lymphedematous limbs included no visu-

alized nodes; a single, large node about 5 cm long; round, fibrotic nodes with homogeneous higher density; multiple small nodules of about 0.5 cm; nodes with an irregular border and homogeneous architecture; irregular nodal outline with homogeneous architecture; and enlarged nodes about 5 to 6 cm with an increased number. Enhanced popliteal nodes were also visualized in two women with primary stage I lymphedema.

Transportation of contrast in lymph nodes. Enhancement of contrast in the inguinal nodes started 30 to 40 minutes after the intracutaneous contrast agent injection. At this time, the inguinal nodes of two healthy volunteers and the limbs without clinical edema were markedly enhanced. A comparison was made of the lymph node/muscle SI ratio between nodes of edematous limbs and contralateral nodes in the normally appearing limbs in 19 patients. The postcontrast MRIs of 34 pairs of nodes showed remark-

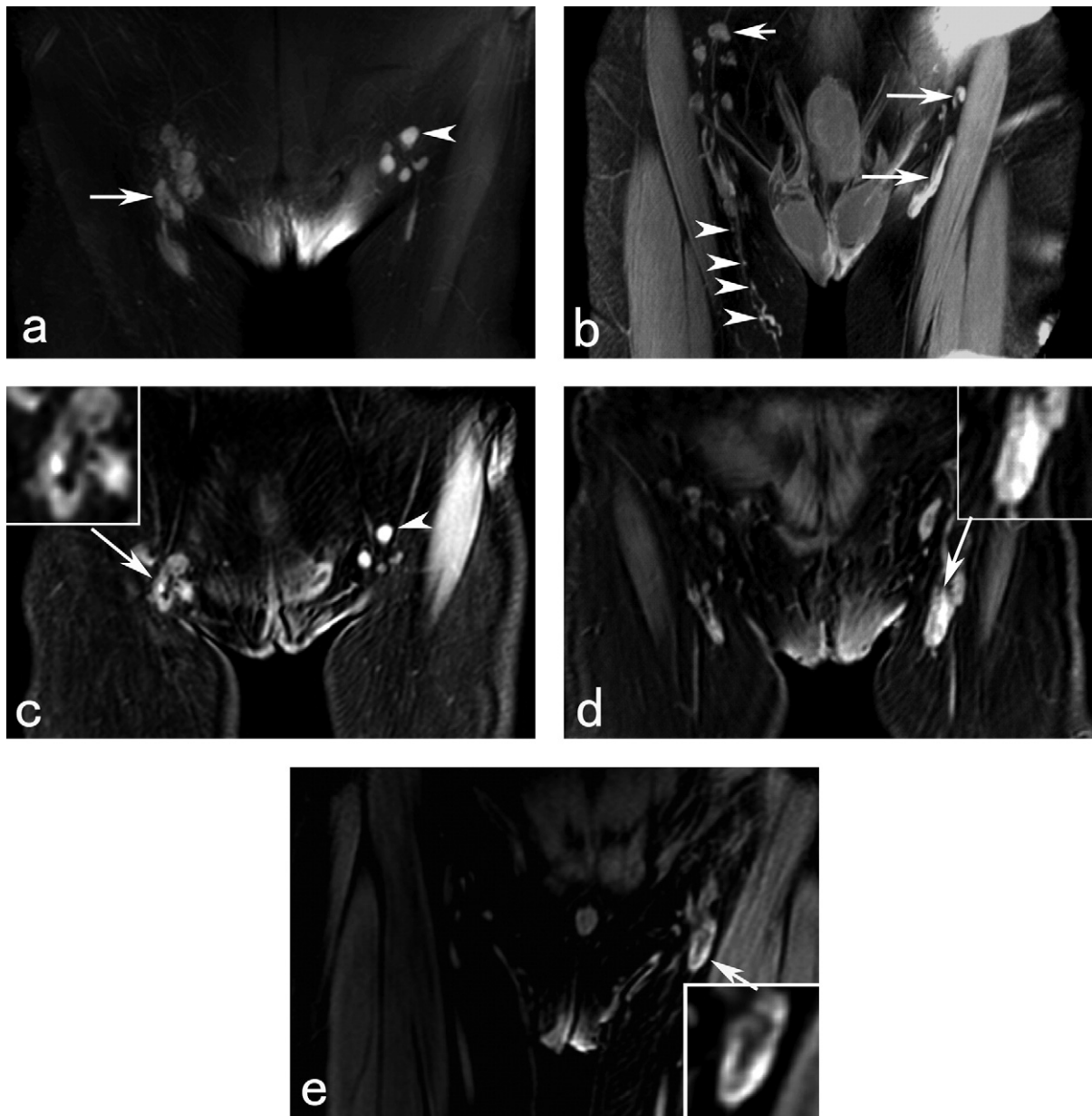


Fig 3. Contrast magnetic resonance lymphangiographic imaging of inguinal lymph nodes. **a**, asymmetrical accumulation of contrast between the nodes with heterogeneous appearance and poor enhancement in the edematous limb (*arrow*) and contralateral nodes that were evenly enhanced (*arrowhead*). **b**, Contrast-enhanced flow is detained in afferent collectors (*arrowheads*) of a limb with lymphangiectasia without enhancement in the drainage nodes (*short arrow*) in contrast to highlighted nodes (*arrow*) in a limb without edema. **c**, Contrast-enhanced central part of nodes (*arrow*) that are irregularly shaped are compared with evenly enhanced contralateral healthy nodes (*arrowhead*). **d**, Central region of the enhanced node with a regular outline in the edematous limb is shown. **e**, Contrast enhancement of contrast in the marginal region of the nodes and left central region unenhanced.

able asymmetrical accumulation of contrast agent between the nodes of edematous limbs and contralateral limbs in patients with unilateral lymphedema (Fig 3, *a*) as well as in the two patients with bilateral lymphedema in whom edema was serious in one limb and mild in the other. The node/muscle SI ratio in lymphedematous limbs after con-

trast enhancement was also significantly lower than in contralateral limbs ($P < .01$). The exception was one patient with Klippel-Trenaunay syndrome, in whom an increased number of enlarged inguinal nodes (about 5 cm in length) and increased contrast enhancement in these large nodes compared with contralateral nodes was seen.

Contrast MR lymphangiography images also displayed varied patterns of contrast material passing through and accumulating within inguinal nodes of 19 patients with lymphedema limbs. A constant homogeneous signal loss in the inguinal node was found in four patients (4/19); in three patients, this was due to total fibrosis of the nodes; and in one patient, it was caused by the contrast material stagnating in the extremely dilated prenodal lymphatic collectors and not reaching the nodes during the test (Fig 3, *b*). In two patients, contrast enhancement appeared mainly in the central zone of the nodes, giving a heterogeneous appearance (Fig 3, *c* and *d*). In nine patients, contrast enhancement was mainly in the marginal region of the nodes while the central region of the nodes remained unenhanced (Fig 3, *e*).

Dynamic contrast-enhanced MRIs of inguinal lymph nodes were also available in nine patients. Wash-in and wash-out curves derived from designated ROIs in 14 pairs of nodes displayed a decreased slope and slower wash-out (Fig 4, *a*), remarkable reduced peak enhancement ($P < .01$, Fig 4, *b*), and a significantly longer time to peak enhancement ($P < .01$, Fig 4, *c*) in the edematous limbs.

DISCUSSION

In this study, we present for the first time an analysis of contrast MR lymphangiography with gadobenate dimeglumine in the diagnosis of lymphatic circulation disorders. This test provided a quick and accurate method of visualizing the lymphatic pathway and lymph nodes in lymphedematous limbs. Lymphatic vessels in a limb with lymph flow disturbances were visualized, but the lymphatic vessels in a healthy limb were not. This might be due to the faster flow speed of lymph in the healthy limb. Thus, lymph circulation disorders should be suspected when contrast-enhanced lymphatics are visualized with this test.

Transportation of the contrast agent by the draining lymphatic system and regional lymph nodes also allowed a consecutive and real-time inspection of the transport function of the lymphatic system and the lymph nodes within a reasonable length of time. Furthermore, the specificity of absorption and transportation of the contrast agent by the lymphatic system allowed visualization of detailed morphologic changes of lymphatic vessels and regional lymph nodes by using high-resolution MRIs. Finally, quantitative assessment of abnormal lymph flow kinetics was achieved by tracing the flow within the lymphatic vessels and comparing dynamic nodal enhancement and time-signal intensity curves between edematous and contralateral limbs.

This combination of the lymphatic and lymph node images may outline the integral picture of the affected lymphatic system. Because of its advantages compared with the conventional diagnostic method for lymphedema of lymphoscintigraphy and noncontrast MRI, contrast MR lymphangiography is now the routine diagnostic tool for lymphedema in our clinic. The comprehensive information provided by contrast MR lymphangiography not only helps in the differential diagnosis of lymphedema from other

types of peripheral edema but also enhances our understanding of the pathophysiology of lymphostatic diseases.

Shortly after injection, contrast material was absorbed by lymphocytes, and the lymphatic system was visualized in all lymphedematous limbs regardless of disease duration or lymphatic vessel distribution. Thus, there was no failure of contrast agent absorption and transportation in the injection site, indicating no dysfunction at the primary lymphatic level and also demonstrating spontaneous contraction and transportation capability of lymphatic vessels.

Lymph flow in lymphatic channels may be influenced by multiple factors, and the ways pathologic abnormalities influence lymph flow kinetics remain largely unknown. Indeed, MR contrast lymphangiography demonstrated a variety of lymphatic distribution patterns, diameters, and numbers of vessels and nodes in primary lymphedema, which may represent different mechanisms of pathogenesis. Regardless, the causal relationship between lymph flow kinetics and lymphatic system pathologies needs to be determined to allow more direct and effective treatment of lymphedema.

In the lymph node, lymphatic fluid drains from the afferent lymphatic vessels into the marginal sinus, circulates through a complex cortical and medullar sinus network, and exits through the efferent vessel into the blood circulation. Flow resistance is 100 times greater in the lymph nodes than in the lymph collectors.⁸ Lymphatic circulation disorders may be caused solely by lymph node abnormalities, by a lymphatic vessel problem, or a combination of lymphatic and lymph node abnormalities.^{9,10} However, the influence of nodal factors on peripheral lymph flow failure remains unclear. Nodal imaging in nonmalignant lymphostatic diseases has been described in a few reports, and enhanced MR lymphangiography has proved useful for the diagnosing and staging of malignant lymph nodes.^{5-8,11}

The present study shows the usefulness of contrast MR lymphangiography in detecting morphologic and functional abnormalities of draining lymph nodes in benign lymphatic disorders. This included highlighting of the medullar region first, which is the opposite of normal intranodal lymph flow, and enhancement of marginal sinuses regions with central filling defects. In addition, delayed nodal enhancement on was found in 18 of 19 tested cases. The dysfunction of prenodal lymphatic collector transportation may thus play an important role in reduced nodal lymph flow input. However, the decline of nodal enhancement over time, partial nodal enhancement, and changed nodal filling patterns suggest the existence of intranodal pathology. Real-time monitoring of nodal transporting functions showed a significantly longer peak enhancement time, reduced peak enhancement, decreased curve slope, and slower wash-out, which may be direct evidence of nodal involvement in lymphatic circulation failure.

The molecular size of the contrast agent may have important effect in lymphatic imaging.¹² The optimum size that preferentially drains through the lymphatic system remains unclear. The ideal contrast agent for identifying lymphatic pathways and regional lymph nodes would be specially absorbed by the initial lymphatic system, delivered in a high

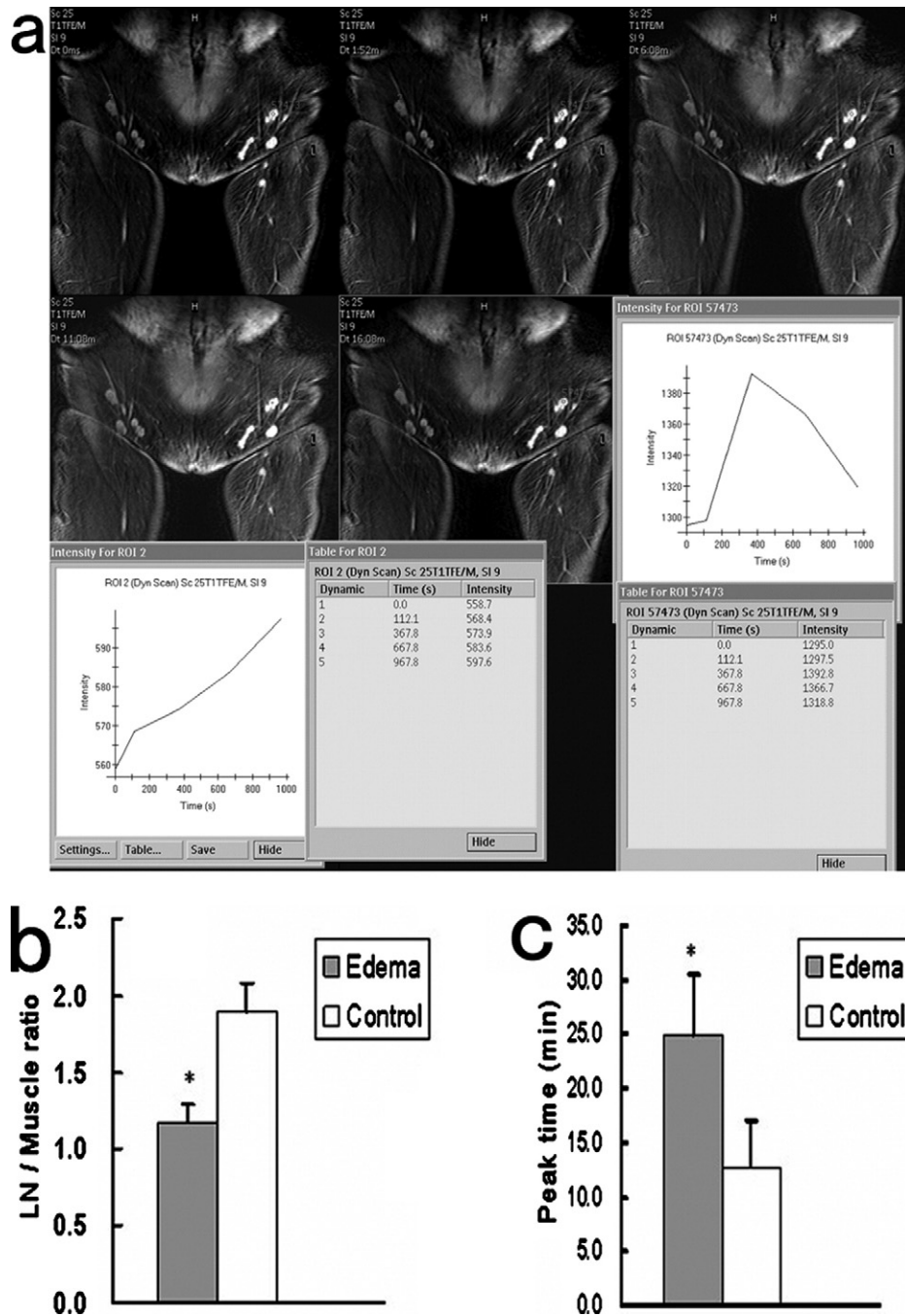


Fig 4. Coronal images of dynamic enhancement of lymph nodes after contrast injection. **a**, Real-time record of comparison of nodal enhancement in edematous (*arrow*) and nonedematous (*arrowhead*) limbs in a series images. The wash-in curve was prolonged in (*left*) the affected limb in contrast with a quick wash-in and wash-out curve in (*right*) the unaffected limb. **b**, Peak time node vs muscle signal intensity ratios ($n = 14$) in affected limbs were significantly lower than that of unaffected limbs. **c**, Nodes of edematous limbs displayed significantly longer time to peak enhancement ($n = 14$). Data are presented as mean with the standard deviation. $P < 0.01$ indicates statistical significance.

concentration to lymph nodes, and would have a low background concentration in the surrounding healthy tissue.

Commonly used radionuclides in the lymphoscintigraphy are macromolecules such as isotope-labeled albumin

(about 60 kDa) and dextran (70 to 80 kDa). These macromolecular contrast agents are passively absorbed by the terminal lymphatic system through the open junctions of endothelial cells.¹³ However, sometimes superficial lym-

phatic collecting ducts in the lymphedematous limb are not visualized by lymphoscintigraphic imaging when these agents are used.^{13,14} This may be due to stasis of the isotopic contrast in the injection site or dysfunction at the initial lymphatic level.

The paramagnetic contrast agent we used in this study to visualize the anatomy and physiology of superficial extremity lymphatic vessels and draining lymph nodes was gadobenate dimeglumine, a micromolecular weight (about 1 kDa) contrast agent. It has special properties that may allow differential targeting of lymphatic vessels and uptake by lymph nodes.¹⁵ Good uptake was demonstrated in both draining lymphatic and regional nodes after intracutaneous injection. This agent also provided good visualization of lymphatic vessels and lymph nodes and an excellent, specific, signal-to background ratio.

The precise mechanism of uptake of gadobenate dimeglumine by lymphatic vessels and lymph nodes is not understood. The agent probably drains from the dermal to lymphatic pathway through thin-walled lymphatic vessels and gaps between endothelial cells. This depends on a combination effect of hydrostatic pressure, osmosis, and volumes, similar to other extracellular, water-soluble, low-molecular solutes.^{16,17} The visualization of individual nodes may be related to slow transit and sequestration of the contrast material in each node.¹³ It is currently unknown whether use of a micromolecular or a macromolecular contrast agent produces different imaging results.

Because this is a preliminary study, there are many areas for future research. It would be useful to determine the pathogenesis of each functional lymphatic system abnormality detected by MR lymphangiography, particularly for abnormalities associated with regional lymph nodes. It would also be useful to compare the effects of using a micromolecular contrast agent with a macromolecular agent in MR lymphangiography. Finally, it would be interesting to study whether initial absorption and transportation of macromolecules by lymphatic vessels can be accurately tested by using micromolecular contrast MR imaging.

CONCLUSIONS

We present a useful modality for imaging the extremity lymphatic system in patients with lymphedema. Contrast MR lymphangiography with gadobenate dimeglumine was able to visualize the precise anatomy of lymphatic vessels and lymph nodes in lymphedematous limbs. This method is minimally invasive, is easy and safe to use, and combines morphologic and functional examinations in a single process. The comprehensive information provided by contrast MR lymphangiography can be used to characterize the lymphatic system in a limb with lymph circulation disorders and may be useful in staging and classification of primary lymphostatic diseases and assessment of the response to treatment.

We extend our thanks to Bin-Shun Wang, director of the Department of Statistics, Shanghai Jiao Tong University School of Medicine, for statistical analysis.

AUTHOR CONTRIBUTIONS

Conception and design: NL
Analysis and interpretation: NL, QL, CW
Data collection: NL, QL, ZJ, JZ
Writing the article: NL, QL
Critical revision of the article: NL
Final approval of the article: NL
Statistical analysis: NL
Obtained funding: NL
Overall responsibility: NL

REFERENCES

1. Liu NF, Wang CG. The role of magnetic resonance imaging in diagnosis of peripheral lymphatic disorders. *Lymphology* 1998;31:119-27.
2. Liu NF, Wang CG, Sun MH. Non-contrast three-dimensional magnetic resonance imaging vs lymphoscintigraphy in the evaluation of lymph circulation disorders: a comparative study. *J Vasc Surg* 2005;41:69-75.
3. Barrett T, Choyke PL, Kobayashi H. Imaging of the lymphatic system: new horizons. *Contrast Med Mol Imaging* 2006;1:230-45.
4. Bellin MF, Lebleu L, Meric JB. Evaluation of retroperitoneal and pelvic lymph node metastases with MRI and MR lymphangiography. *Abdom Imaging* 2003;28:155-63.
5. Al-Nahhas A, Win Z, Al-Sayed Y, Khan S, Sinch A, Rubello D, et al. Anatomic and functional imaging in the management of lymphoma. *Q J Med Mol Imaging* 2007;51:251-9.
6. Kobayashi H, Kawamoto S, Brechbiel MW, Bernardo M, Sato N, Waldmann TA, et al. Detection of lymph node involvement in hematologic malignancies using micromagnetic resonance lymphangiography with a gadolinium-labeled dendrimer nanoparticle. *Neoplasia* 2005;7:984-91.
7. Kobayashi H, Kawamoto S, Bernardo M, Brechbiel MW, Knopp MV, Choyke PL. Delivery of gadolinium-labeled nanoparticles to the sentinel lymph node: comparison of the sentinel node visualization and estimations of intra-nodal gadolinium concentration by the magnetic resonance imaging. *J Control Release* 2006;111:343-51.
8. Kubik S. Anatomy of the lymphatic system. In: Foldi M, Foldi E, Kubik S. *Textbook of lymphology*. München: Elsevier GmbH; 2003. p. 34-5.
9. Kinmonth JB, Eustace PW. Lymph nodes and vessels in primary lymphoedema. *Ann R Coll Surg Engl* 1976;58:278-84.
10. Kinmonth JB, Wolfe JH. Fibrosis in the lymph nodes in primary lymphoedema, histological and clinical studies in 74 patients with lower-limb oedema. *Ann R Coll Surg Engl* 1980;62:344-54.
11. Harisinghani MG, Saksena MA, Hahn PF, King B, Kim J, Torabi M, et al. Ferumoxtran-10-enhanced MR lymphangiography: does contrast-enhanced imaging alone suffice for accurate lymph node characterization? *AJR Am J Roentgenol* 2006;186:144-8.
12. Kobayashi H, Kawamoto S, Choyke PL, Sato N, Knopp MV, Waldmann TA, et al. Comparison of dendrimer-based macromolecular contrast agents for dynamic micro-magnetic resonance lymphangiography. *Magn Reson Med* 2003;50:758-66.
13. Pecking AP, Alberini JL, Wartski M, Edeline V, Cluzan RV. Relationship between lymphoscintigraphy and clinical findings in lower limb lymphedema (LO): toward a comprehensive staging. *Lymphology* 2008;41:1-10.
14. Brice G, Mansour S, Bell R, Collin JRO, Child AH, Brady AF, et al. Analysis of the phenotypic abnormalities in lymphedema-distichiasis syndrome in 74 patients with FOXC2 mutations or linkage to 16q64. *J Med Genet* 2002;39:478-83.
15. Suga K, Yuan Y, Ogasawara N, Okada M, Matsunaga N. Visualization of normal and interrupted lymphatic drainage in dog legs with interstitial MR lymphography using an extracellular MR contrast agent, gadopentetate dimeglumine. *Invest Radiol* 2003;38:349-5.
16. Ruehm SG, Corot C, Debatin JF. Interstitial MR lymphography with a conventional extracellular gadolinium-based agent: assessment in rabbits. *Radiology* 2001;218:664-9.
17. Ruehm SG, Schroeder T, Debatin JF. Interstitial MR lymphangiography with gadoterate meglumine: initial experience in humans. *Radiology* 2001;220:816-21.

Submitted Jun 26, 2008; accepted Nov 7, 2008.